Microburst Scale Size Derived from a Bouncing Packet Microburst Simultaneously Observed with the FIREBIRD-II CubeSats

Mykhaylo Shumko[1], John Sample[1], Arlo Johnson[1], Bern Blake[2], Alex Crew[3], Harlan Spence[4], David Klumpar[1], Oleksiy Agapitov[5], Matthew Handley[1]

[1]Department of Physics, Montana State University, Bozeman, MT
[2]Space Science Applications Laboratory, The Aerospace Corporation, Los Angeles, California
[3]The Johns Hopkins University Applied Physics Laboratory LLC, Laurel, Maryland
[4]Institute for the Study of Earth, Oceans, and Space, University of New Hampshire, Durham, NH
[5]Space Sciences Laboratory, UC Berkeley, Berkeley, CA

Key Points:

- A bouncing packet microburst was simultaneously observed by the two FIREBIRD-II CubeSats on February 2nd, 2015.
- The microburst's latitudinal and longitudinal scale sizes at LEO was $> 28.8 \pm 0.8$ km and $> 38.5 \pm 8.8$ km, respectively.
- The microburst LEO scale sizes mapped to the magnetic equator are $> 504 \pm 14$ km radially, and $> 451 \pm 103$ km azimuthally.

Values need to be confirmed To-do

Corresponding author: Mykhaylo Shumko, msshumko@gmail.com

Abstract

Max 150 words, describe the problem we are trying to solve The FIREBIRD-II CubeSats simultaneously observed a bouncing packet microburst on February 2nd, 2015 during a small storm. It is believed to be the largest microburst observed, with a latitudinal scale size of $> 28.8 \pm 0.8$ km and the longitudinal scale size $> 38.5 \pm 8.8$ km at low earth orbit, assuming a soft energy spectra. Using the Tsyganenko 1989 magnetic field model, these scale sizes were mapped to the magnetic equator to get the radial and azimuthal scale sizes of $> 504 \pm 14$ km and $> 451 \pm 103$ km, respectively, assuming a soft energy spectra. The magnetospheric location and conditions, and the similarity of the microburst and whistler-mode chorus scale sizes at the magnetic equator reported in previous literature indicate that this microburst was probably scattered by a whistler-mode chorus wave. Lastly, the electron bounce period of the subsequent bounces was calculated and compared to analytical and numerical bounce times. There was good agreement for high energy electrons, but there was as much as $\sim 20\%$ difference at the lowest energies that FIREBIRD-II can detect. These results will hopefully guide future electron loss, magnetic field, and wave-particle interaction models. In addition, future multi-spacecraft missions will be necessary to extend on the distribution of microburst scale sizes from the few microbursts that were simultaneously observed with FIREBIRD-II.

1 Introduction

The dynamics of the radiation belt electrons is complex, and is driven by interactions between source and loss mechanisms. A few loss mechanisms include radial diffusion [*Shprits and Thorne*, 2004], pitch-angle diffusion [*Selesnick et al.*, 2003], magnetopause shadowing [*Ukhorskiy et al.*, 2006], and pitch angle scattering from wave-particle interactions. As described in [*Millan and Thorne*, 2007; *Thorne*, 2010] and references contained within, there are a variety of waves that cause pitch angle scattering, including EMIC waves, Plasmaspheric Hiss, ULF waves, and whistler-mode chorus. Whistler-mode chorus predominantly occur in the dawn sector [*Li et al.*, 2009] and is believed to accelerate electrons with large equatorial pitch angles[*Horne and Thorne*, 2003]. It is currently believed that chorus waves cause an intense increase in electron precipitation flux termed microbursts.

Microbursts are observed in Low Earth Orbit (LEO) [*Nakamura et al.*, 1995, 2000; *Blake et al.*, 1996; *Lorentzen et al.*, 2001a,b; *O'Brien et al.*, 2003, 2004; *Blum et al.*, 2015; *Crew et al.*, 2016], and similarly to chorus waves, they predominantly occur in the dawn sector [*Lorentzen et al.*, 2001b]. For this analysis, a microburst is defined by a greater than one order of magnitude increase in electron flux on the time scale of $\sim$ 100 ms. Understanding microburst precipitation is important to radiation belt dynamics since they have been theorized and empirically estimated to deplete the relativistic electron population of the outer radiation belt on time scales of hours to a few days [*O'Brien et al.*, 2004; *Thorne et al.*, 2005; *Shprits et al.*, 2007].

For the last $\sim$ 2.5 years, microbursts have been observed by the FIREBIRD-II (FB) pair of CubeSats (FU3 and FU4) at LEO. On February 2nd, 2015, a bouncing packet microburst was simultaneously observed on both spacecraft. The microburst decay was observed over the period of a few seconds, while the spacecraft were traversing in L. This analysis uses FU3 and FU4 to resolve the space-time ambiguity of the microburst. The rest of this paper is organized as follows: in section 2, the spacecraft and the microburst observation will be introduced. In section 3, the methodology of the spacecraft time and position correction, the microburst latitudinal and longitudinal scale sizes in LEO and the magnetic equator, and electron bounce period will be explained. Lastly, in section 4, these results will be tied to the current empirical and theoretical understanding of microbursts.

2 Spacecraft and Observation

FB is an identically-instrumented pair of 1.5 U CubeSats (FU3 and FU3), launched on January 31st, 2015. Their polar orbit has an apogee of 632 km and perigee of 433 km, and 99.1° inclination [*Crew et al.*, 2016]. FB is mostly sampling in L shell, with a small precession in MLT. FU3 and FU4 are flying in a leader-follower configuration with FU4 ahead, to resolve the space-time ambiguity inherent to single spacecraft missions such as SAMPEX.

Each FB unit has a collimated and a surface solid state detectors with complementary fields of view of 45° and 180°, respectively. They are observing electron precipitation in six energy channels from $\sim$ 230 keV to $>$ 1 MeV. The adjustable cadence can be as high as 12.5 ms [*Crew et al.*, 2016].

On February 2nd, 2015 at 06:12:50 UT, a microburst with subsequent bounces was observed simultaneously on both spacecraft. Figure 1 shows the 18.75 ms cadence flux data (HiRes) of the bouncing packet microburst. Five peaks were observed on FU3, and four peaks were observed on FU4. On the collimted detector, the microburst was seen up to the fourth energy channel (555 - 771 keV), while on the surface detector it was observed up to the fifth energy channel (683 - 950 keV). Only FU3 has a functioning surface detector, thus only data from the lowest four energy channels of the collimated detectors will be used for this analysis.

We believe this to be a single miroburst since the first peak is not dispersed, but subsequent peaks show some dispersion. In addition, no microbursts were observed for 8 s before the event and there was very little flux. This microburst was observed at McLlwain L = 4.7, MLT = 8.3, calculated using the Tsyganenko 1989 (T89) magnetic field model [*Tsyganenko*, 1989] with the IRBEM library. This event occurred above Sweden, latitude = 63°, longitude = 15°, altitude = 650 km, at the eastern edge of the bounce loss cone. Lastly, the magnetosphere was mildly disturbed with Kp = 4, and DST = -44 nT, during the transition between the main and recovery phases.

3 Analysis

3.1 Time and position correction

At the beginning of the FB mission, there was uncertainty in their separation and their clocks were not synchronized. Our approach to calculate their time difference, δt_e and separation, δt_d is a cross-correlation time lag analysis on events that are temporal and spatial. It is believed that these spatial structures are stationary from similar structures observed from $>$ 35 keV to a few hundred keV on the AC-6 CubeSats and their position confirmed with GPS [*Blake and O'Brien*, 2016]. The time lag of a spatial structure, Δt is a combination of the clock difference, and the time of flight difference due to spacecraft separation. It is related via,

$$\Delta t = \delta t_d + \delta t_e. \tag{1}$$

Six coincident microbursts, and two spatial events around this microburst were hand-picked on February 2nd, 2015 for this analysis. The coincident microbursts were linearly fit to account for clock drift and a clock difference of $\delta t_e = 2.28 \pm 0.12\ s$ was obtained. This time shift was applied to the HiRes data in Fig. 1. The cross-correlation analysis on the two spatial events yields a time lag of $\Delta t = 4.92 \pm 0.03$ s. Using these values, and the Two Line Elements (TLE) derived spacecraft velocity, $v = 7.57\ km/s$ the calculated spacecraft separation was,

$$d = v\ \delta t_d = 19.9 \pm 0.9\ km. \tag{2}$$

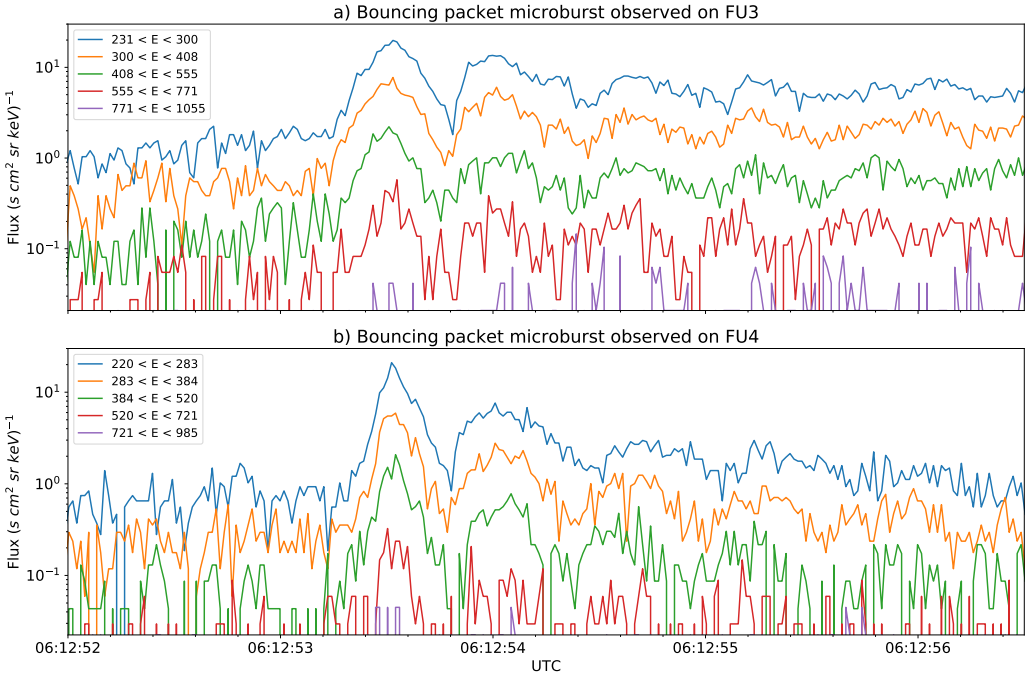

Figure 1. HiRes data of the bouncing packet microburst observed at February 2nd, 2015 at 06:12:50 UT. The subsequent bounces show little energy dispersion. The energy channels' label unit is keV. As discussed in section 3 a time correction of -2.28 s has been applied to FU3. While we show flux from five non-integral channels, the flux from the highest non-integral energy channel has little counts for reliable analysis.

An independent method to confirm the cross-correlation derived separation and timing difference was developed. The separation was calculated using TLEs. The TLE released for February 2nd, was anomalous and was not used. Instead, we backpropagated seven TLEs released up to five days after the microburst event, and propagated them with the SGP-4 algorithm. Then the predicted spacecraft separations at the time of the microburst event were averaged to derive a separation of $d = 18.38 \pm 1.47$ km. The timing difference was calculated using the time stamps of the FB telemetry beacons during operational passes. Since they had a common time reference, the ground station computer, a time difference $\delta t_e = 2.45^{+0.98}_{-0.51}$ s was derived. These two methods give similar results, which imply that the stationary event assumption used in the cross-correlation time lag analysis, is in fact, a decent assumption.

3.2 Microburst Scale Sizes

Using the $\sim$ 20 km in-track separation, and the spacecraft motion during the event, microburst scale sizes in LEO and the magnetic equator are calculated. Using the event and orbit topology shown in Fig. 2 and error propagated from the spacecraft separation, the latitudinal scale size is $> 28.8 \pm 0.8$ km. This scale size is represented by the latitudinal extent of the solid and dashed boxes in Fig. 2.

Since magnetospheric electrons drift eastward and were seen for multiple bounces, it is possible to calculate the longitudinal scale size of the microburst. The distance that the electrons drift azimuthally in a single bounce is given by,

$$d_{az} = 2\pi(R_E + A)\cos(\lambda)\frac{t_b}{< T_d >} \tag{3}$$

where R_E is the Earth's radius, A is the spacecraft altitude, λ is the magnetic latitude, t_b is the electron bounce period, and $< T_d >$ is the electron drift period. *Parks* [2003] derived $< T_d >$ to be,

$$< T_d > \approx \begin{cases} 43.8/(L \cdot E) & \text{if } \alpha_0 = 90^\circ \\ 62.7/(L \cdot E) & \text{if } \alpha_0 = 0^\circ \end{cases} \tag{4}$$

where E is the electron energy is MeV, L is the L shell, and α_0 is the equatorial pitch angle. The valid limit for this analysis is $\alpha_0 = 0^\circ$ since electrons mirroring at FB have $\alpha_0 \approx 3.7^\circ$.

Since FB saw multiple bounces after the microburst, the longitudinal scale size is the furthest distance that the microburst electrons drifted and were last seen. This was calculated with $D_{az} = n\ d_{az}$ where n is the number of bounces observed. Using this methodology, the longitudinal scale size is $> 38.5 \pm 8.8\ km$ for the 555 keV electrons and $> 50.8 \pm 11.4\ km$ for the 771 keV electrons. The stars with energy labels in Fig. 2 represent the locations of electrons with that energy when the microburst was seen at the first peak (P1), and drifted eastward to be last seen at P5 for FU3 and P4 for FU4.

The longitudinal and latitudinal scale sizes at LEO were mapped to the magnetic equator using the T89 magnetic field model. The mapped radial scale size (latitudinal scale mapped from LEO) is $> 504 \pm 14$ km and azimuthal scale size (longitudinal scale mapped from LEO) of 555 keV electrons is $> 451 \pm 103$ km and of 771 keV electrons is $> 530 \pm 119$ km.

3.3 Electron Bounce Period

Lastly, the observed bounce period, t_b as a function of energy is calculated. To calculate the observed t_b and uncertainties, the HiRes flux was detrended and fitted. The detrening flux (baseline) is defined in *O'Brien et al.* [2004] as the flux at the 10th percentile over a time interval around the point to be detrended. A 0.5 s interval is used in this analysis. The flux was fitted with five Gaussians for FU3, and four for FU4. The fit uncertainty is from the detrended flux and the baseline flux summed in quadrature. Using the fit parameters, the mean t_b for the lowest four energy channels was calculated and shown in Fig. 3 with rectangles.

Superposed on Fig. 3, are t_b curves for various models including an analytical solution from *Schulz and Lanzerotti* [1974], and numerical models: T89, Tsyganenko 2005 (T05) [*Tsyganenko and Sitnov*, 2005], and Olson & Pfitzer Quiet [*Olson and Pfitzer*, 1982]. The numerical t_b curves were calculated using a Python wrapper for IRBEM that traces the magnetic field line between mirror points, one of which is set at FB and calculates t_b via

$$t_b = 2 \int_{m_s}^{m_n} \frac{ds}{v_{||}(E, s)} \tag{5}$$

where m_n and m_s are the northern and southern mirror points along a field line that is parameterized by s. The electron parallel velocity, $v_{||}(E, s)$ is calculated at each point along the field line assuming conservation of the first adiabatic invariant.

4 Discussion

The scale sizes reported in section 3.2 are a lower bound. They are similar to the latitudinal scale size reported in *Blake et al.* [1996] where SAMPEX observed a bouncing packet microburst on October 4th, 1992, and shown in Fig. 6 in *Blake et al.* [1996]. Furthermore, the latitudinal scale size in this study is roughly $\sim$ 2.6 times larger than other simultaneous microbursts reported in *Crew et al.* [2016].

From section 3.2, the microburst scale size at the magnetic equator is similar to the whistler-mode chorus source scale sizes reported in *Agapitov et al.* [2011, 2017]. In *Agapitov et al.* [2011], chorus source scale scales of $\sim$ 600 km were observed by CLUSTER at $L \sim 4.5$. In *Agapitov et al.* [2017], RBSP was used to measure source scale sizes of $\sim$ 500

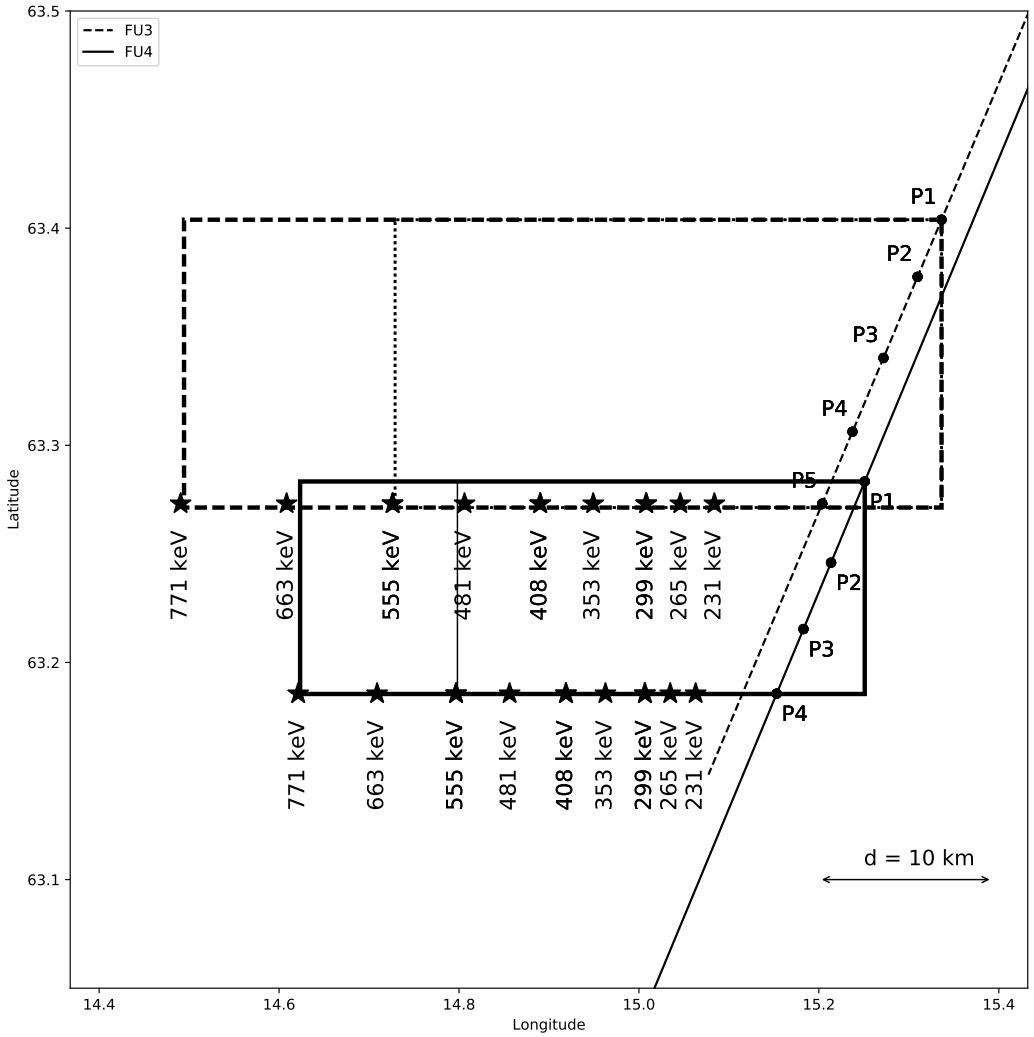

148 **Figure 2.** The topology of the FB orbit and the bouncing packet microburst projected onto latitude and
149 longitude with axis scaled to equal distance. Attributes relating to FU3 shown with dashed lines, and FU4
150 with solid lines. The spacecraft path is shown with the diagonal lines, starting at the upper right corner. The
151 labels P(N) indicate where the spacecraft were when the N^{th} peak was seen in the lowest energy channel in
152 the HiRes data. The stars with the accompanying energy labels represent the locations of the electrons with
153 that energy that started at time of P1, and were seen at the last peak on each spacecraft. The thick (thin) box
154 represents the upper (lower) bound on the microburst scale size, assuming that the majority of the electrons
155 were in the upper (lower) boundary of energy channel 4.

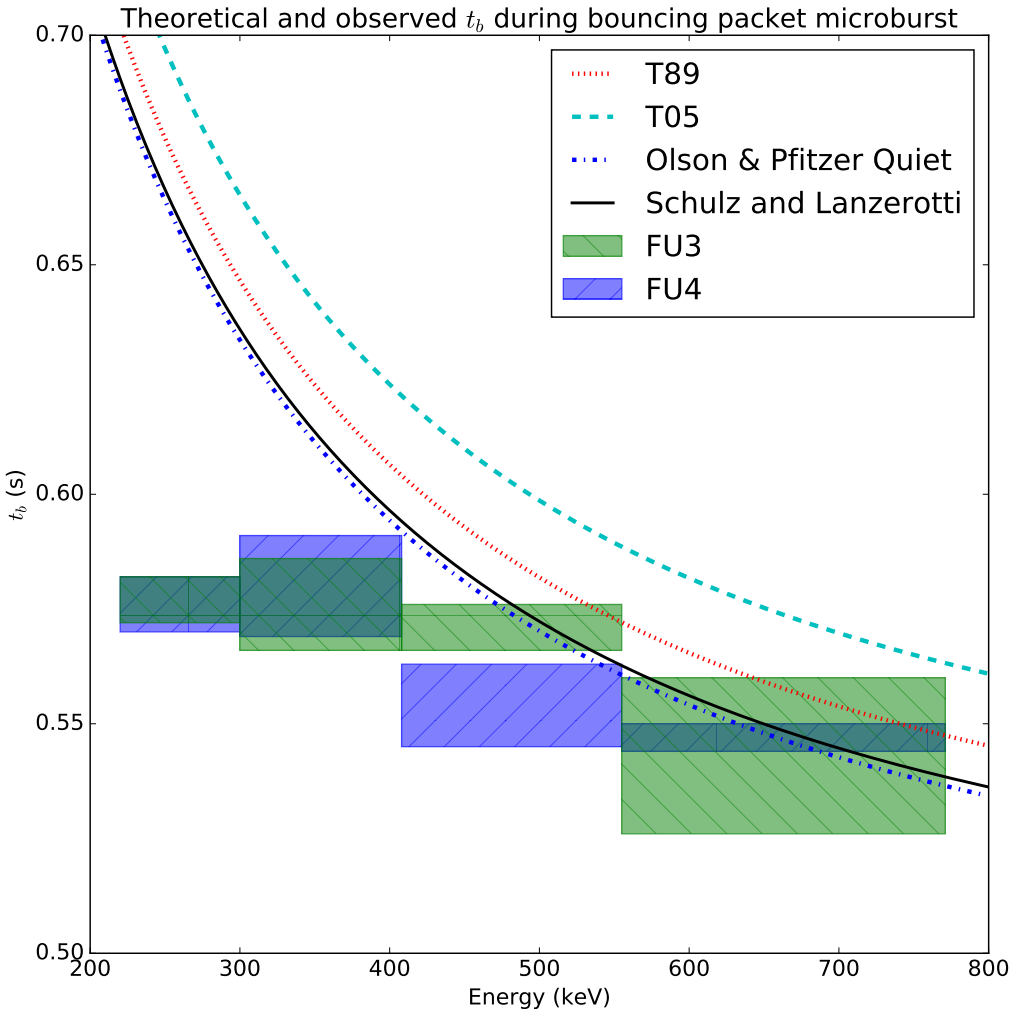

Figure 3. Observed and theorized t_b for electrons of energies from 200 to 770 keV. The solid black line is t_b in a dipole magnetic field, derived in *Schulz and Lanzerotti* [1974]. The red and cyan dashed lines are the t_b derived using the T89, and T05 magnetic field models with IRBEM. Lastly, the blue dashed curve is the t_b derived using the Olson & Pfitzer Quiet model. The green and blue boxes represent the observed t_b for FU3 and FU4, respectively. The width of the boxes represent the width of those energy channels, and the height represents the uncertainty from the fit.

and $\sim$ 800 km for upper and lower band chorus, respectively. This mapping relies on the assumption that the interaction occurred at the magnetic equator. It is possible that the microburst electrons were scattered off the equator [*Lorentzen et al.*, 2001b], but it is outside the scope of this analysis to discern the magnetic latitude of the interaction. From the similarity in scale sizes, magnetospheric location, and geomagnetic conditions, it is possible that this microburst was scattered by a whistler-mode chorus.

Using the fit parameters from section 3.3, the exponential E-folding energy, E_0 is calculated. It is found to be $E_0 \sim 100\ keV$, which is soft for a typical microburst observed with FB, so the lower bound of the scale would be closer to the 555 keV electrons. There is no statistically significant change in E_0 for subsequent bounces.

Lastly, as shown in Fig. 3, while the observed high energy t_b agree well to most models, T05 seems to be the worst at predicting the bounce period. To get an estimate of the discrepecy, the input position for the T05 is adjusted to give better agreement with the observed t_b. The adjusted L shell is smaller by $\Delta L = 0.35$. At the lower energies where there is a larger discrepancy the models differ by as much as $\sim 20\%$.

5 Conclusions

The bouncing packet microburst observed by both FB CubeSats shed light on the spatial and temporal properties of microbursts in LEO and the magnetic equator region. We believe that it is the largest observed, with a latitudinal scale size of $> 28.8 \pm 0.8$ km and the longitudinal scale size $> 38.5 \pm 8.8$ km at LEO, assuming a soft energy spectra. Using the T89 magnetic field model, these scale sizes were mapped to the magnetic equator. The radial scale size is $> 504 \pm 14$ km and azimuthal scale size is $> 451 \pm 103$ km, assuming a soft energy spectra. The similarity of the derived microburst equatorial scale size to the whistler-mode chorus source region scale size, magnetospheric location, and geomagnetic conditions indicate that the microburst electrons were probably scattered by a whistler-mode chorus wave.

Lastly, the observed and theoretical bounce periods match up decently at high energies, but disagree by as much as $\sim 20\%$ at the lowest energies that FB can detect.

Hopefully, these results will guide future modeling efforts in areas not limited to: estimating particle loss from the radiation belts, wave-particle interactions, and magnetic field modeling. Lastly, this microburst's scale sizes are a lower bound, and there is a distribution of microburst scale sizes. While a study to quantify the distribution of microburst scale sizes using FB is currently under way, FB saw a small number of coincident microbursts before they were too far apart. To derive a more robust distribution of microburst scale sizes, a FB-like mission with station keeping abilities will be necessary to increase the satellite's exposure to microbursts while controlling their separation.

Acknowledgments

I acknowledge the FIREBIRD team, and the members of the Space Sciences and Engineering Laboratory at MSU for their hard work to make this mission a success. In addition, I acknowledge Drew Turner for his suggestions regarding the bounce period calculations. This material is based upon work at Montana State University supported by the National Science Foundation under Grant Numbers 0838034 and 1339414.

References

Agapitov, O., V. Krasnoselskikh, T. Dudok de Wit, Y. Khotyaintsev, J. S. Pickett, O. Santolik, and G. Rolland (2011), Multispacecraft observations of chorus emissions as a tool for the plasma density fluctuations' remote sensing, *Journal of Geophysical Research: Space*

Physics, *116*(A9), n/a–n/a, doi:10.1029/2011JA016540, a09222.

Agapitov, O., L. W. Blum, F. S. Mozer, J. W. Bonnell, and J. Wygant (2017), Chorus whistler wave source scales as determined from multipoint van allen probe measurements, *Geophysical Research Letters*, pp. n/a–n/a, doi:10.1002/2017GL072701, 2017GL072701.

Blake, J., M. Looper, D. Baker, R. Nakamura, B. Klecker, and D. Hovestadt (1996), New high temporal and spatial resolution measurements by sampex of the precipitation of relativistic electrons, *Advances in Space Research*, *18*(8), 171 – 186, doi: http://dx.doi.org/10.1016/0273-1177(95)00969-8.

Blake, J. B., and T. P. O'Brien (2016), Observations of small-scale latitudinal structure in energetic electron precipitation, *Journal of Geophysical Research: Space Physics*, *121*(4), 3031–3035, doi:10.1002/2015JA021815, 2015JA021815.

Blum, L., X. Li, and M. Denton (2015), Rapid mev electron precipitation as observed by sampex/hilt during high-speed stream-driven storms, *Journal of Geophysical Research: Space Physics*, *120*(5), 3783–3794, doi:10.1002/2014JA020633, 2014JA020633.

Crew, A. B., H. E. Spence, J. B. Blake, D. M. Klumpar, B. A. Larsen, T. P. O'Brien, S. Driscoll, M. Handley, J. Legere, S. Longworth, K. Mashburn, E. Mosleh, N. Ryhajlo, S. Smith, L. Springer, and M. Widholm (2016), First multipoint in situ observations of electron microbursts: Initial results from the nsf firebird ii mission, *Journal of Geophysical Research: Space Physics*, *121*(6), 5272–5283, doi:10.1002/2016JA022485, 2016JA022485.

Horne, R. B., and R. M. Thorne (2003), Relativistic electron acceleration and precipitation during resonant interactions with whistler-mode chorus, *Geophysical Research Letters*, *30*(10), n/a–n/a, doi:10.1029/2003GL016973, 1527.

Li, W., R. M. Thorne, V. Angelopoulos, J. Bortnik, C. M. Cully, B. Ni, O. LeContel, A. Roux, U. Auster, and W. Magnes (2009), Global distribution of whistler-mode chorus waves observed on the themis spacecraft, *Geophysical Research Letters*, *36*(9), n/a–n/a, doi:10.1029/2009GL037595, l09104.

Lorentzen, K. R., J. B. Blake, U. S. Inan, and J. Bortnik (2001a), Observations of relativistic electron microbursts in association with vlf chorus, *Journal of Geophysical Research: Space Physics*, *106*(A4), 6017–6027, doi:10.1029/2000JA003018.

Lorentzen, K. R., M. D. Looper, and J. B. Blake (2001b), Relativistic electron microbursts during the gem storms, *Geophysical Research Letters*, *28*(13), 2573–2576, doi: 10.1029/2001GL012926.

Millan, R., and R. Thorne (2007), Review of radiation belt relativistic electron losses, *Journal of Atmospheric and Solar-Terrestrial Physics*, *69*(3), 362 – 377, doi: http://dx.doi.org/10.1016/j.jastp.2006.06.019, global Aspects of Magnetosphere-Ionosphere CouplingGlobal Aspects of Magnetosphere-Ionosphere Coupling.

Nakamura, R., D. N. Baker, J. B. Blake, S. Kanekal, B. Klecker, and D. Hovestadt (1995), Relativistic electron precipitation enhancements near the outer edge of the radiation belt, *Geophysical Research Letters*, *22*(9), 1129–1132, doi:10.1029/95GL00378.

Nakamura, R., M. Isowa, Y. Kamide, D. Baker, J. Blake, and M. Looper (2000), Observations of relativistic electron microbursts in association with vlf chorus, *J. Geophys. Res*, *105*, 15,875–15,885.

O'Brien, T. P., K. R. Lorentzen, I. R. Mann, N. P. Meredith, J. B. Blake, J. F. Fennell, M. D. Looper, D. K. Milling, and R. R. Anderson (2003), Energization of relativistic electrons in the presence of ulf power and mev microbursts: Evidence for dual ulf and vlf acceleration, *Journal of Geophysical Research: Space Physics*, *108*(A8), n/a–n/a, doi: 10.1029/2002JA009784, 1329.

O'Brien, T. P., M. D. Looper, and J. B. Blake (2004), Quantification of relativistic electron microburst losses during the gem storms, *Geophysical Research Letters*, *31*(4), n/a–n/a, doi:10.1029/2003GL018621, l04802.

Olson, W. P., and K. A. Pfitzer (1982), A dynamic model of the magnetospheric magnetic and electric fields for july 29, 1977, *Journal of Geophysical Research: Space Physics*, *87*(A8), 5943–5948, doi:10.1029/JA087iA08p05943.

Parks, G. (2003), *Physics Of Space Plasmas: An Introduction, Second Edition*, Westview Press.

Schulz, M., and L. J. Lanzerotti (1974), *Particle Diffusion in the Radiation Belts*, Springer.

Selesnick, R. S., J. B. Blake, and R. A. Mewaldt (2003), Atmospheric losses of radiation belt electrons, *Journal of Geophysical Research: Space Physics*, *108*(A12), doi: 10.1029/2003JA010160, 1468.

Shprits, Y. Y., and R. M. Thorne (2004), Time dependent radial diffusion modeling of relativistic electrons with realistic loss rates, *Geophysical Research Letters*, *31*(8), n/a–n/a, doi:10.1029/2004GL019591, l08805.

Shprits, Y. Y., N. P. Meredith, and R. M. Thorne (2007), Parameterization of radiation belt electron loss timescales due to interactions with chorus waves, *Geophysical Research Letters*, *34*(11), n/a–n/a, doi:10.1029/2006GL029050, l11110.

Thorne, R. M. (2010), Radiation belt dynamics: The importance of wave-particle interactions, *Geophysical Research Letters*, *37*(22), doi:10.1029/2010GL044990, l22107.

Thorne, R. M., T. P. O'Brien, Y. Y. Shprits, D. Summers, and R. B. Horne (2005), Timescale for mev electron microburst loss during geomagnetic storms, *Journal of Geophysical Research: Space Physics*, *110*(A9), n/a–n/a, doi:10.1029/2004JA010882, a09202.

Tsyganenko, N. (1989), A solution of the chapman-ferraro problem for an ellipsoidal magnetopause, *Planetary and Space Science*, *37*(9), 1037 – 1046, doi: http://dx.doi.org/10.1016/0032-0633(89)90076-7.

Tsyganenko, N. A., and M. I. Sitnov (2005), Modeling the dynamics of the inner magnetosphere during strong geomagnetic storms, *Journal of Geophysical Research: Space Physics*, *110*(A3), n/a–n/a, doi:10.1029/2004JA010798, a03208.

Ukhorskiy, A. Y., B. J. Anderson, P. C. Brandt, and N. A. Tsyganenko (2006), Storm time evolution of the outer radiation belt: Transport and losses, *Journal of Geophysical Research: Space Physics*, *111*(A11), n/a–n/a, doi:10.1029/2006JA011690, a11S03.